

Depth-Structured Music Recurrence: Budgeted Recurrent Attention for Full-Piece Symbolic Music Modeling

Yungang Yi^{a,*}, Weihua Li^a, Matthew Kuo^a, Catherine Shi^a, Quan Bai^b

^aAuckland University of Technology, Auckland, New Zealand

^bUniversity of Tasmania, Tasmania, Australia

Abstract

Long-context modeling is essential for symbolic music generation, since motif repetition and developmental variation can span thousands of musical events, yet practical workflows frequently rely on resource-limited hardware. We introduce Depth-Structured Music Recurrence (DSMR), a training-time design that learns from complete compositions end to end by streaming each piece left-to-right with stateful recurrent attention and distributing layer-wise memory horizons under a fixed recurrent-state budget. Our main instantiation, two-scale DSMR, assigns long history windows to lower layers and a uniform short window to the remaining layers. On the MAESTRO piano performance dataset, two-scale DSMR matches a full-memory recurrent reference in perplexity (5.96 vs. 5.98) while using approximately 59% less GPU memory and achieving roughly 36% higher throughput. Variant analyses further show strong layer substitutability under binary-horizon schedules: performance depends primarily on total allocated memory rather than which layers carry it.

Keywords: Symbolic music generation, Long-context modeling, Recurrent attention, Streaming training, Depth-Structured Music Recurrence

1. Introduction

Musical coherence depends on context that spans many bars or entire compositions: motif repetition, phrase development, and sectional form can stretch across thousands of symbolic events [1, 2]. At the same time, practical music creation and on-device experimentation often operate under tight compute and memory budgets. Efficient long-context modeling is therefore central to realistic symbolic music generation.

Transformer self-attention is effective for sequence modeling but scales quadratically with length [3], making it a dominant bottleneck for long musical streams. Although subquadratic alternatives, e.g., sparse attention [4, 5], linear attention [6], and state-space models [7], reduce per-step cost, they do not address a separate, equally important problem: *training-time context fragmentation*. Standard language-model pipelines truncate long sequences into fixed-length excerpts and optimize them as independent samples [8]. This windowed regime is convenient for batching, yet it systematically fragments piece-level structure in symbolic music, where salient phenomena routinely span an entire composition.

Segment-level recurrence, as introduced by Transformer-XL [9], offers a natural remedy: by caching key/value (KV) states across segments, the model can condition on long-range history without recomputing the preceding segments. However,

standard recurrent Transformers treat cross-segment memory as a uniform, fixed-window cache at every layer. This uniform allocation is wasteful: not all depths require the same amount of history, and retaining full-length memory at every layer is prohibitively expensive on consumer-grade hardware.

In this paper, we propose **Depth-Structured Music Recurrence (DSMR)**, a training-time design that makes full-piece end-to-end learning feasible under constrained resources. DSMR streams each composition through stateful recurrent attention and distributes layer-wise memory horizons under a fixed total recurrent-state budget, so that different layers access different amounts of past context. Our main instantiation is a **two-scale DSMR** schedule: lower layers retain long history windows while the remaining layers share a uniform short window. On the MAESTRO piano performance dataset [10], two-scale DSMR matches a full-memory recurrent reference in perplexity (5.96 vs. 5.98) while using approximately 59% less GPU memory and achieving roughly 36% higher throughput. Variant analyses further reveal strong layer substitutability under binary-horizon (selective retention) schedules, indicating that performance depends primarily on how much total memory is allocated rather than which specific layers carry it, and that learned memory-usage gates, while exhibiting non-uniform depth preferences, do not reliably transfer as guidance for choosing memory-carrying layers.

Our contributions are threefold. First, we introduce DSMR as a training-time framework that enables end-to-end learning on complete symbolic music compositions by streaming each piece left-to-right with stateful recurrent attention, where the carried cross-segment states are budgeted through a layer-wise

*Corresponding author.

Email addresses: yungang.yi@aut.ac.nz (Yungang Yi), weihua.li@aut.ac.nz (Weihua Li), matthew.kuo@aut.ac.nz (Matthew Kuo), catherine.shi@aut.ac.nz (Catherine Shi), quan.bai@utas.edu.au (Quan Bai)

horizon schedule so that full-piece training remains feasible under limited compute. Second, we propose two-scale DSMR as the main instantiation: long horizons are allocated to lower layers and a uniform short horizon to the remaining layers, keeping recurrent-state cost within a fixed budget without reducing model depth. Third, we provide systematic variant analyses that characterize the DSMR design space, establishing that depth-wise memory redistribution outperforms binary layer selection at matched budgets, and that gate-derived layer rankings do not reliably transfer under structural intervention.

The remainder of this paper is organized as follows. Section 2 reviews related work. Section 3 presents the DSMR framework and its two-scale instantiation. Section 4 describes the experimental setup. Section 5 reports the main results and variant analyses. Section 6 discusses implications, scope conditions, and limitations.

2. Related Work

We review prior work along four axes: subquadratic attention mechanisms, stateful recurrence with budgeted memory, layer-wise memory optimization, and long-context symbolic music modeling.

2.1. Subquadratic Long-Context Mechanisms

A large body of work reduces attention cost through sparsity or approximation. Representative approaches include sparse/block attention [4], sliding-window and global-token schemes [5], sparse graph-style attention [11], and kernelized/linearized attention [6, 12]. Beyond attention modifications, selective state-space models such as Mamba achieve linear-time sequence modeling with input-dependent state updates [7], and hybrid architectures such as Titans augment attention with persistent memory modules [13]. At the system level, sparse attention mechanisms optimized for long-context LLM efficiency have also been proposed [14]. These methods reduce per-step cost but are complementary to the training-time concern addressed by DSMR: even with efficient attention, standard pipelines still fragment long sequences into fixed-length excerpts, discarding piece-level structure.

2.2. Recurrent Transformers and Budgeted Stateful Memory

Complementary to subquadratic attention, long-context modeling can be achieved via stateful recurrence, where hidden states from previous segments are cached and reused as additional attention context. Transformer-XL introduced segment-level recurrence with cached activations and relative positional encoding, enabling dependencies beyond a fixed window while reducing context fragmentation [9]. Its segment-bounded compute makes it particularly attractive for streaming workloads, and it serves as the recurrent backbone adopted by DSMR. However, standard Transformer-XL uses a uniform, fixed-length memory window at every layer and deterministically discards states beyond that window; DSMR departs from this design by assigning layer-wise horizons so that different depths retain different amounts of history.

Building on Transformer-XL-style recurrence, several budgeted mechanisms extend history under limited memory. Compressive Transformer summarizes older states into a lower-resolution buffer, trading fidelity for longer temporal coverage [15]. Recurrent Memory Transformer (RMT) carries learned memory slots across segments [16], and ERNIE-Doc augments recurrence with extended history and a retrospective feed to strengthen cross-segment information flow [17]. These approaches budget memory through compression or fixed-size slots, whereas DSMR budgets memory by redistributing per-layer horizons under a fixed total.

An inherent concern with cached cross-segment states is staleness: as the number of recurrent steps grows, earlier cached states become increasingly outdated relative to current parameters. While staleness has been studied in pipelined and asynchronous optimization [18, 19], its impact on training dynamics in full-piece end-to-end music streaming—where a single composition may span over 30 recurrent steps—has not been previously examined.

2.3. Layer-Wise Memory Optimization

Recurrent Transformers carry key/value states across segments as a persistent KV cache. This cache is often redundant across depth, with substantial inter-layer similarity in cached states [20]. Motivated by this, inference-time studies on non-recurrent Transformers examine layer-wise KV-cache utility, showing it is heterogeneous across depth and making uniform budgeting suboptimal: SqueezeAttention assigns layer-wise KV budgets based on sensitivity [21], LAVa derives dynamic layer (and head) budgets from information-loss considerations [22], and MiniCache exploits depth-wise redundancy by compressing highly similar KV states across adjacent middle-to-deep layers [20].

Depth heterogeneity also appears in recurrent stacks, where long-range access is provided by stateful memories carried across segments. Notably, Rae et al. [23] show that, for language modeling, better performance can be obtained by limiting the attention/memory range in lower layers, suggesting that long-range memory may be more valuable in higher layers. Our experiments on symbolic music yield the opposite pattern: allocating long horizons to lower layers outperforms allocating them to higher layers, indicating that the preferred depth placement is task-dependent.

Despite these findings, optimizing layer-wise horizon lengths—i.e., non-uniform per-layer memory windows that go beyond binary keep/drop decisions—remains largely unexplored in recurrent settings. DSMR addresses this gap by systematically varying per-layer horizons under a fixed total budget.

2.4. Long-Context Symbolic Music Modeling under Resource Constraints

A central goal in symbolic music generation is to capture long-range structure and full-piece coherence, since motifs, harmonic plans, and section-level returns can span thousands of events. To this end, music-specific long-context models explore structure-aware mechanisms for efficiency and long-term

coherence, including improved relative attention [1], fine-coarse attention over salient vs. nonsalient bars [2], whole-song hierarchical generation using cascaded diffusion models [24], and long-context pretraining for symbolic-music foundation models [25]. LLM-style large-scale symbolic models further raise expectations on coherence and musicality [26].

These architectural advances expand the effective context available to the model. However, in practice, training pipelines in symbolic music generation remain dominated by efficiency-driven recipes: fixed-length segmentation, bounded-context truncation, or hierarchical/cascaded generation with fixed-scope local modeling, rather than end-to-end full-piece training. This parallels common LLM pretraining practice, which constructs fixed-length training sequences for efficiency; the specific sequence composition and masking strategy can meaningfully affect pretraining behavior [27], and Ding et al. [8] show that “concatenate-then-split” can unnecessarily break documents that would otherwise fit within the context window, degrading coherent-content modeling. DSMR targets this gap by training on complete pieces end to end via streaming recurrence, avoiding the structural fragmentation inherent in fixed-length excerpt training.

3. Depth-Structured Music Recurrence (DSMR)

Depth-Structured Music Recurrence (DSMR) is a training-time design for end-to-end full-piece symbolic music modeling via streaming recurrence. DSMR streams each composition left-to-right with stateful recurrent attention; under a fixed recurrent-state budget, it allocates depth-dependent (layer-wise) memory horizons to constrain the cost of carrying cross-segment states without reducing model depth. Our final instantiation is a **two-scale DSMR** schedule: long horizons in lower layers and a uniform short horizon elsewhere.

3.1. Recurrent backbone

We adopt a Transformer-XL style segment-level recurrence. Each layer caches past key/value states and reuses them as additional attention context for subsequent segments. Unlike Transformer-XL, which discards older segments beyond a fixed window, DSMR ensures that at least one layer retains full-length (maximum-horizon) memory so that long-range context is never deterministically discarded; the specific layer(s) carrying long memory may differ across model variants. For completeness, details of Transformer-XL recurrence and its approximation to full self-attention are provided in Appendix Appendix A. Fig. 1 illustrates the segment-level recurrence with cached history and discarded context beyond the horizon.

3.2. Training-time sampling and segmentation

DSMR trains with full-piece sampling: each training example is an entire musical piece processed sequentially from the first segment to the last. Let a piece be partitioned into segments $\{x^{(t)}\}_{t=1}^T$. For each segment t , the model computes attention for the current tokens using queries from $x^{(t)}$ over a context formed by concatenating the current segment with cached

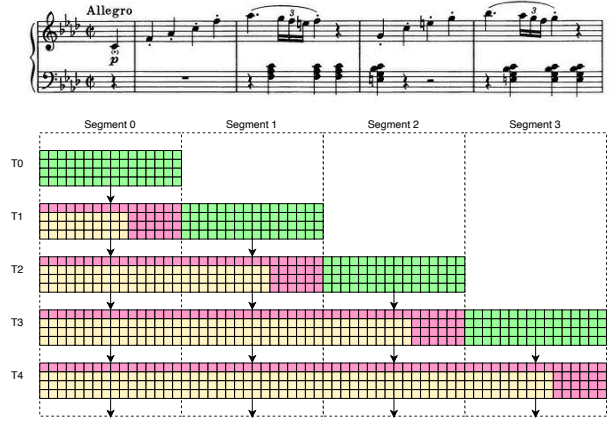


Figure 1: **Full-piece segment-level recurrence.** Attention for the current segment (green) is computed using its own tokens together with cached key/value states from all previous history (red). The history horizon is managed on a layer-wise basis; in our two-scale DSMR schedule, some memory is discarded (yellow).

key/value states from all preceding segments. In other words, the current segment attends to the full available history through the recurrent cache, so long-range context is provided without deterministically discarding earlier segments.

For data augmentation, we randomize the length of the first segment by sampling its token length from a predefined range, while all subsequent segments use a fixed length. This introduces variable starting offsets for the same piece while keeping the recurrent training schedule and compute profile stable for the remainder of the sequence.

3.3. Full-attention approximation of a vanilla Transformer as a reference model

Transformer-XL enforces a fixed uniform horizon m by retaining only the most recent m cached states via the following memory update [9], so attention to history is limited to a sliding window:

$$M_t^n = \text{SG}\left(\left[M_{t-1}^n; H_{t-1}^n\right]_{-m}\right), \quad (1)$$

Appendix Appendix A.1 provides the exact stateful recurrent attention formulation for Transformer-XL, including memory concatenation, truncation, and stop-gradient across segments.

To approximate full-length context, DSMR extends Transformer-XL by setting the horizon to the maximum available prefix length for all layers, yielding a full-memory recurrent model.

Because DSMR uses truncated backpropagation through time (BPTT) with a stop-gradient across segments, it induces a biased approximation to full self-attention over the entire prefix, since the cached states are produced by parameters from earlier optimization steps. Let θ denote the current parameters, and let θ_{old} denote the parameters that produced the cached states. Then the recurrent attention uses history states computed by earlier parameters,

$$(K_{\text{cache}}, V_{\text{cache}}) = (K(\theta_{\text{old}}), V(\theta_{\text{old}})), \quad (2)$$

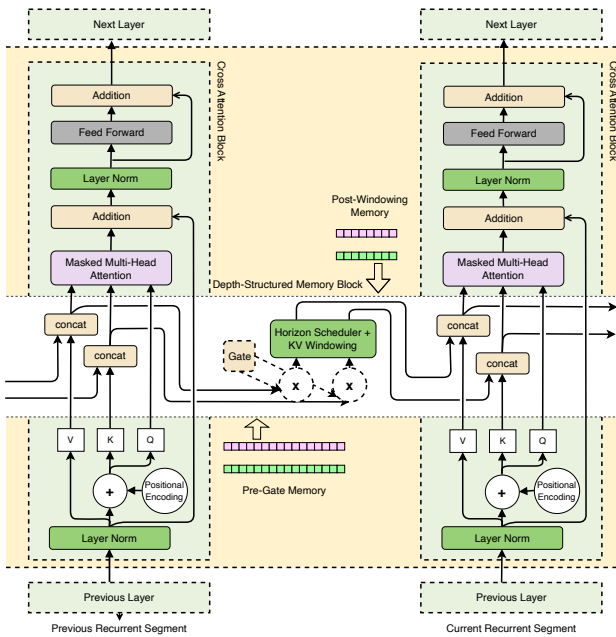


Figure 2: **Depth-Structured Music Recurrence (DSMR)** in a recurrent layer. Key/value states from previous segments flow forward as a history buffer and are truncated by a layer-specific horizon to satisfy a fixed memory budget. The retained history is concatenated with the current segment’s key/value context to form the attention source for that layer.

whereas full self-attention over the prefix would (in principle) use states computed consistently under the current parameters,

$$(K_\theta, V_\theta) = (K(\theta), V(\theta)). \quad (3)$$

We can express the resulting parameter-mismatch effect as

$$(K_{\text{cache}}, V_{\text{cache}}) = (K_\theta, V_\theta) + (\Delta K, \Delta V), \quad (4)$$

where $(\Delta K, \Delta V)$ captures the discrepancy due to reusing cached states produced by earlier parameters. We analyze the implications of this staleness for optimization stability in Sec. 6.2.

Removing time-axis truncation provides a practical approximation to full self-attention in a vanilla Transformer, while retaining the computational benefits of segment-wise processing; Appendix Appendix A.2 analyzes this approximation.

3.4. Layer-wise horizon schedules

Beyond a uniform global horizon, DSMR enforces layer-wise horizons $\{m^{(\ell)}\}$, so different depths see different amounts of history, which shapes recurrent attention into depth-dependent receptive fields. DSMR uses two types of schedules: binary-horizon schedules, where $m^{(\ell)} \in \{0, m_0\}$ and only a subset of layers carry memory (studied as a model variant); and redistributive schedules, where memory is present across depths but horizons vary by layer under a fixed total budget (our main approach). Fig. 2 depicts the recurrent memory pathway in a layer, including horizon-based truncation and concatenation with the current segment context.

For binary-horizon schedules, let \mathcal{L}_{mem} be the retained-memory layer set with $|\mathcal{L}_{\text{mem}}| = B$ ($B \leq L$), and define

$$m^{(\ell)} = \begin{cases} m_0, & \ell \in \mathcal{L}_{\text{mem}}, \\ 0, & \ell \notin \mathcal{L}_{\text{mem}}. \end{cases} \quad (5)$$

For redistributive schedules, DSMR is specified by a non-negative horizon vector $\mathbf{m} = \{m^{(\ell)}\}_{\ell=1}^L$, where $m^{(\ell)}$ is the memory horizon at layer ℓ . Different horizons across depth define layer-wise temporal receptive fields, inducing depth-dependent recurrent attention. We constrain DSMR under a fixed overall recurrent-state budget:

$$\sum_{\ell=1}^L m^{(\ell)} = M_{\text{tot}}, \quad m^{(\ell)} \geq 0. \quad (6)$$

Under the same M_{tot} , DSMR changes where long-range history is accessible across depth without increasing compute depth or modifying the Transformer block.

3.5. Two-scale schedule

Let $\mathcal{L}_{\text{long}} = \{1, \dots, L_{\text{long}}\}$ denote the lower-layer set. We assign a long horizon to lower layers and a standard short horizon to the remaining layers:

$$m^{(\ell)} = \begin{cases} m_{\text{long}}, & \ell \in \mathcal{L}_{\text{long}}, \\ m_{\text{short}}, & \ell \notin \mathcal{L}_{\text{long}}, \end{cases} \quad (7)$$

$$L_{\text{long}} m_{\text{long}} + (L - L_{\text{long}}) m_{\text{short}} = M_{\text{tot}}. \quad (8)$$

Here m_{long} assigns full-length (maximum-horizon) memory to the designated lower layer(s) to concentrate long-range access, while m_{short} is set by the matched total budget M_{tot} : after allocating m_{long} , we evenly distribute the remaining horizon budget across the other layers. This yields a clear multi-receptive-field pattern: lower layers carry long-range history, and higher layers operate with a shorter recurrent window.

4. Experimental Setup

This section specifies datasets, models, training, and evaluation protocols.

4.1. Datasets and tokenization

We conduct experiments on the MAESTRO dataset, a large-scale collection of virtuosic piano performances with MIDI note events [10]. We filter the dataset to retain only samples whose tokenized lengths fall between 1024 (the segment length) and 32768 tokens (the maximum context length), ensuring every piece spans at least one full segment and fits within the recurrence horizon. We use the train/validation/test split produced by our preprocessing pipeline (0.89/0.10/0.01), and train an autoregressive model over tokenized symbolic event sequences derived from MIDI.

We encode each MIDI performance into an event-based token sequence (note-on, note-off, time-shift, and velocity events, plus special tokens) with vocabulary size $|\mathcal{V}| = 393$.

4.2. Model and recurrence configuration

The model has $L = 18$ layers, hidden size $d = 1024$, $h = 16$ attention heads (with $d_{\text{head}} = 64$), and FFN size $d_{\text{ff}} = 4d = 4096$. Each piece is streamed left-to-right in segments of length $s = 1024$ using the recurrent backbone described in Sec. 3.1, with per-layer memory horizons $\{m^{(\ell)}\}_{\ell=1}^L$ for the recurrent KV cache. Each layer ℓ maintains a recurrent KV memory capped at $m^{(\ell)}$ tokens, with a per-layer maximum of $m_0 = 31744$ tokens. We fix the overall recurrent-state budget to $M_{\text{tot}} = 95232$ (i.e., 31744×3), so varying $\{m^{(\ell)}\}$ redistributes where along depth long-range history is accessible under the same total memory.

Final model: two-scale DSMR (long lower + uniform short elsewhere). We use the **two-scale DSMR** schedule in Eq. (7). We set $L_{\text{long}} = 1$ and $L_{\text{short}} = 17$ (so $L = 18$), where the bottom L_{long} layer uses a long horizon $m_{\text{long}} = 31744$, and the remaining L_{short} layers share a uniform short horizon $m_{\text{short}} = 3734$.

4.3. Variant schedules

We study depth-wise allocation of recurrent memory by instantiating DSMR with several horizon schedules under matched budgets. All variants share the same backbone architecture and training setup; they differ only in the per-layer horizon vector $\{m^{(\ell)}\}_{\ell=1}^L$ and (optionally) a lightweight memory gate. Fig. 3 illustrates the layer-wise horizon allocations for all variants.

Binary-horizon DSMR (selective layer retention). We instantiate DSMR with a binary horizon vector, where only B layers retain recurrent memory and the rest have zero horizon.

We evaluate a memory-depth budget of $B = 3$ and compare different constructions of \mathcal{L}_{mem} under this fixed budget: (i) sliding-window subsets (a contiguous depth window of B layers, shifted to form variants), (ii) uniform subsets (approximately evenly spaced B layers), and (iii) random subsets (sample B layers uniformly at random from the remaining subsets, excluding those that form a sliding-window or uniform construction).

Gate-guided layer selection. As a comparison variant in the binary-horizon setting, we attach a learnable soft gate $g_t^{(\ell)} \in [0, 1]$ to each memory-retained layer, scaling only the historical KV memory contribution during training. Let $(K_{\text{mem},t}^{(\ell)}, V_{\text{mem},t}^{(\ell)})$ denote the recurrent memory at segment t for layer ℓ , and $(K_t^{(\ell)}, V_t^{(\ell)})$ the current-segment keys/values. The gated attention context is

$$\begin{aligned} K_{\text{ctx},t}^{(\ell)} &= [g_t^{(\ell)} K_{\text{mem},t}^{(\ell)} ; K_t^{(\ell)}], \\ V_{\text{ctx},t}^{(\ell)} &= [g_t^{(\ell)} V_{\text{mem},t}^{(\ell)} ; V_t^{(\ell)}], \end{aligned} \quad (9)$$

and attention is computed using $(K_{\text{ctx},t}^{(\ell)}, V_{\text{ctx},t}^{(\ell)})$ in place of the ungated concatenation. We train the gated model, rank layers by mean gate usage $\bar{g}^{(\ell)}$ to select the top- B layers as \mathcal{L}_{mem} , and retrain the resulting selective-retention model for comparison against the heuristic constructions under the same B . We

also evaluate an STE discretization variant [28, 29]: after 250k steps, each gate is binarized to $\{1.0, 0.0\}$ (open/closed), and the resulting binary pattern defines an alternative \mathcal{L}_{mem} .

Progressive depth-dependent caps (redistribution variant). To isolate redistribution effects under a fixed budget, we additionally evaluate a progressive DSMR schedule where $m^{(\ell)}$ varies monotonically with depth, either increasing (larger horizons in deeper layers and smaller horizons in shallow layers) or decreasing (the reverse ordering), while keeping $\sum_{\ell} m^{(\ell)} = M_{\text{tot}}$ fixed.

Reversed two-scale schedule. In addition to the default two-scale DSMR schedule (long horizons in lower layers with a uniform short horizon elsewhere), we also evaluate its reversed counterpart, where the deeper layers adopt the long horizon and the remaining layers use the same short horizon.

Perceiver-AR-like schedule. Perceiver AR achieves long-context modeling by performing cross-attention between the current segment queries and a long key-value memory: the queries come from the short attention segment, while the K/V states are computed by projecting token embeddings from the concatenated context sequence [30]. Appendix Appendix A.3 provides a detailed explanation. Motivated by this design, our Perceiver-AR-like schedule retains full-length (maximum-horizon) recurrent memory only at the shallowest layer, and sets the recurrent horizon of all higher layers to zero (i.e., no cross-segment memory), so higher layers perform only within-segment self-attention.

4.4. Training details

We use Adam with $\beta_1 = 0.9$, $\beta_2 = 0.999$, and $\epsilon = 10^{-8}$. Unless noted, we use the Transformer learning-rate schedule

$$\text{lr}(t) = \text{LR}_0 d^{-1/2} \min(t^{-1/2}, t w^{-3/2}), \quad (10)$$

with warmup $w = 10000$ and $\text{LR}_0 = 1.0$. This gives a peak learning rate $\text{lr}_{\text{max}} = \text{LR}_0 / \sqrt{d w} = 3.125 \times 10^{-4}$ for $d = 1024$. We take one optimizer step per segment. We do not apply gradient clipping and use a cross-attention prefix dropout of 0.1. All experiments run on CUDA-enabled consumer-grade GPUs.

4.5. Evaluation protocol and metrics

Our primary metric is perplexity (PPL) on the validation set:

$$\text{PPL} = \exp\left(\frac{1}{n} \sum_{i=1}^n -\log p(x_i | x_{<i})\right). \quad (11)$$

Unless stated otherwise, we report Best Val PPL at the checkpoint with the lowest validation loss. We also report the compute efficiency (throughput) and cost (wall-clock time and peak memory) in absolute terms for both our models and the full-memory (untruncated-horizon) Transformer-XL-style recurrent reference, to characterize the budget-quality tradeoff.

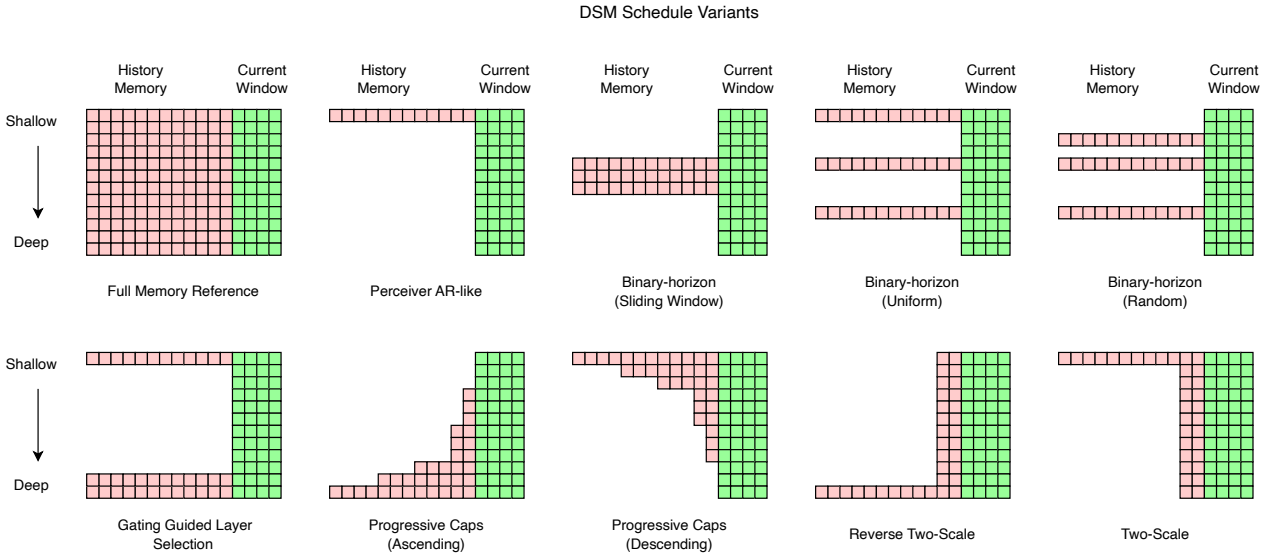


Figure 3: Layer-wise memory-horizon schedules (allocations) for DSMR variants.

Table 1: Key hyperparameters used in our experiments.

Item	Value
Layers L	18
Hidden size d	1024
Heads h	16
FFN size d_{ff}	4096
Segment length s	1024
Per-layer cap m_0	31744 ($= 32768 - s$)
Memory-depth budgets B	3

5. Results

We present results in three parts: (i) quality and efficiency of DSMR schedules against baselines under matched recurrent-state budgets; (ii) layer substitutability under binary-horizon (selective retention) schedules; and (iii) whether learned memory-usage gates provide actionable guidance for layer selection.

5.1. Quality–efficiency tradeoff

We compare all DSMR schedules and baselines under the matched budget $M_{\text{tot}} = Bm_0$ ($B=3$), with a full-memory reference as an unconstrained upper bound (Sec. 4.2). Figure 4 summarizes the quality–budget tradeoff. Under comparable memory usage ($\sim 6\text{--}8$ GB), the two-scale DSMR schedule achieves the lowest Best Val PPL among budgeted methods (5.96), outperforming gate-guided selective retention (6.53) and the Perceiver-AR-like reference (6.54), while the full-memory reference attains 5.98 at substantially higher memory cost (15.5 GB). Under a fixed recurrent-state budget, redistributing horizons across all depths is more effective than concentrating memory in a small subset of layers.

Table 2 additionally reports training efficiency. The two-scale DSMR schedule uses 59.1% less GPU memory and trains 26.4% faster (wall-clock time to best checkpoint) than the full-memory reference, while matching its Best Val PPL (5.96 vs. 5.98).

5.2. Layer substitutability under selective retention

We evaluate the binary-horizon DSMR variant (selective retention) to test whether performance depends on which depths carry recurrent memory when the depth budget B is fixed. We compare sliding-window, uniform-spacing, and random retained-layer subsets \mathcal{L}_{mem} , where $m^{(\ell)} = m_0$ for $\ell \in \mathcal{L}_{\text{mem}}$ and $m^{(\ell)} = 0$ otherwise.

Table 2 shows that performance varies little across subset patterns (Best Val PPL: sliding-window 6.51, uniform 6.52, random 6.53). This indicates strong structural substitutability: within our setting, performance is largely determined by the number of layers with nonzero horizons (the budget B), rather than which specific layers carry memory.

5.3. Gate preferences versus transferable importance

We then study whether learned memory usage provides actionable guidance for allocating memory retention across layers. When we equip memory-carrying layers with a learnable gate $g^{(\ell)}$ (Sec. 4.3), gate dynamics exhibit overall shrinkage together with increasing differentiation across depth during training: $\text{KL}_{\text{uniform}}$ increases over steps, while gate entropy and the effective number of active layers decrease (Figure 5).

These trends persist even without an explicit global gate budget or binarization regularization. In late training (after 250k steps), applying a Straight-Through Estimator (STE) [28, 29] drives gates toward a near-discrete regime (open/closed) (Figure 7), while without STE gates remain continuous but still separate across depth (Figure 6).

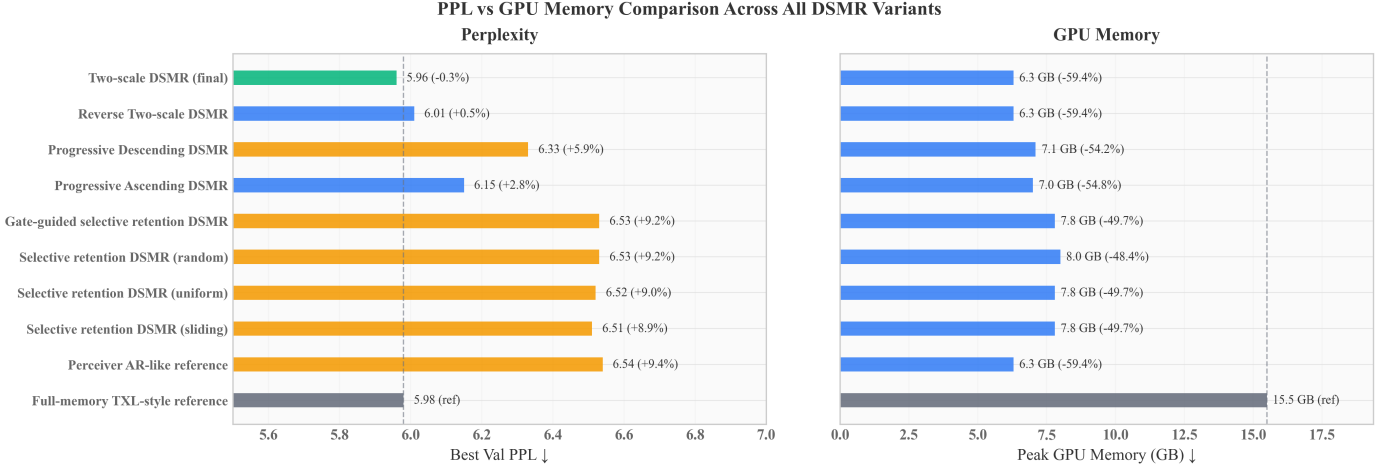


Figure 4: Best validation perplexity (PPL) versus peak GPU memory across DSMR variants, with full attention as a reference.

Table 2: Efficiency metrics on MAESTRO. All runs see 15,098,825 training tokens. Percentages in parentheses are relative to the full-attention reference. Bold indicates the best value among non-full-attention methods.

Setting	Tokens/s	Peak GPU Mem (GB)	Time to best checkpoint (h)	Best Val PPL
Full-memory TXL-style reference	7,618	15.5	6.06	5.98
Perceiver AR-like reference	11,753 (+54.3%)	6.3 (-59.1%)	3.92 (-35.3%)	6.54 (+9.4%)
Selective retention DSMR (sliding-window)	11,061 (+45.2%)	7.8 (-49.6%)	4.17 (-31.1%)	6.51 (+9.0%)
Selective retention DSMR (uniform)	11,257 (+47.8%)	7.8 (-49.3%)	4.10 (-32.3%)	6.52 (+9.1%)
Selective retention DSMR (random)	11,160 (+46.5%)	8.0 (-48.0%)	4.13 (-31.9%)	6.53 (+9.3%)
Gate-guided selective retention DSMR	11,141 (+46.2%)	7.8 (-49.7%)	4.14 (-31.7%)	6.53 (+9.2%)
Progressive Ascending DSMR	10,540 (+38.4%)	7.0 (-54.5%)	4.38 (-27.7%)	6.15 (+2.9%)
Progressive Descending DSMR	10,556 (+38.6%)	7.1 (-54.3%)	4.37 (-27.9%)	6.33 (+5.9%)
Reverse Two-scale DSMR	10,324 (+35.5%)	6.3 (-59.1%)	4.47 (-26.2%)	6.01 (+0.5%)
Two-scale DSMR (final)	10,339 (+35.7%)	6.3 (-59.1%)	4.46 (-26.4%)	5.96 (-0.3%)

Notes: Best Val PPL is measured at the checkpoint with the lowest validation loss, and Time to best checkpoint is the wall-clock time elapsed until that checkpoint.

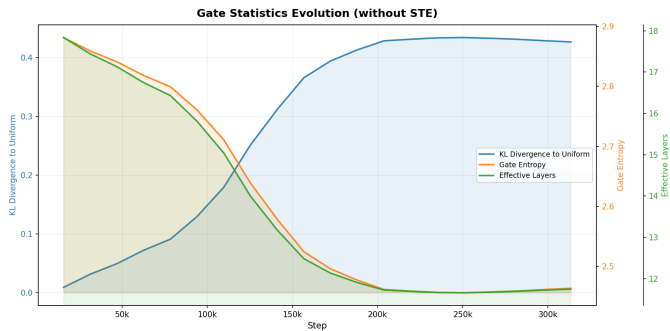


Figure 5: Gate statistics evolution (without STE), showing overall shrinkage and increasing differentiation of gates across depth.

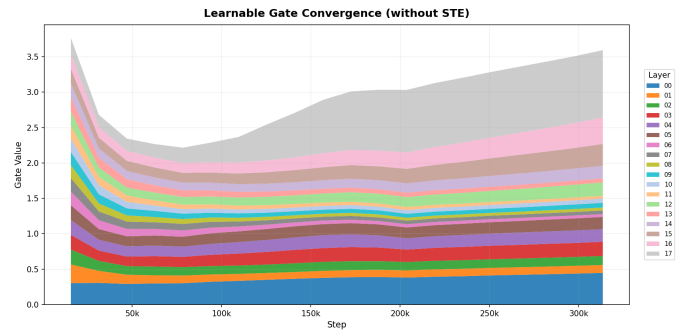


Figure 6: Learnable gate convergence **without STE**. Gates exhibit progressive shrinkage and depth-wise differentiation over training.

Figure 8 reports post-training layer-wise mean gates $\bar{g}^{(\ell)}$. Although gate values are clearly non-uniform across depth, using gate ranking to choose \mathcal{L}_{mem} and retraining under the same depth budget does not yield consistent gains over heuristic layer selections (Table 2). This suggests that gate magnitudes reflect coordination/credit assignment in the original computation graph, rather than transferable causal importance under structural intervention on the layer-wise temporal receptive fields.

6. Discussion

We contextualize our findings from four angles: an information-theoretic perspective on context depth, state staleness under recurrence, practical implications, and limitations.

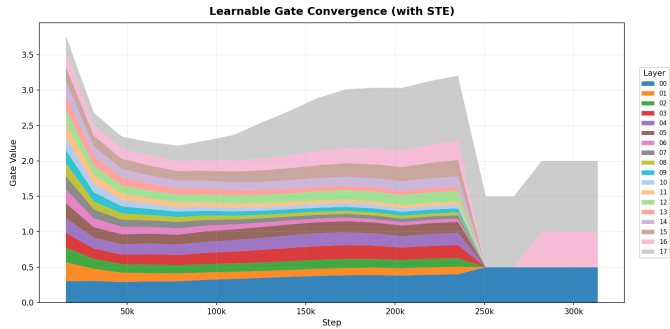


Figure 7: Learnable gate convergence **with** STE. Late-stage STE discretization collapses already-differentiated gates into a near-discrete regime.

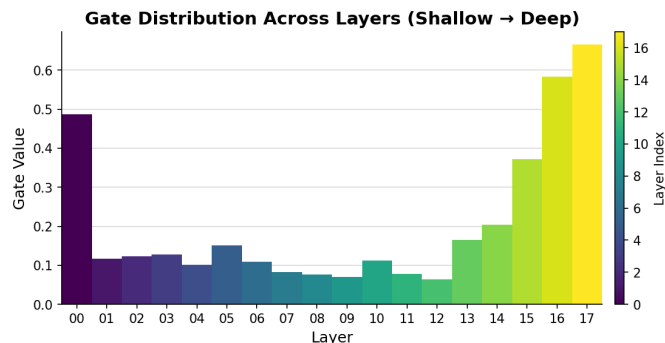


Figure 8: Post-training mean memory-gate values $\bar{g}^{(\ell)}$ across layers (00–17).

6.1. Information-theoretic perspective on context depth

Two information-theoretic observations underpin the DSMR design.

First, longer context cannot worsen the optimal achievable log-loss. If a model class conditioning on context length $L_2 > L_1$ subsumes the predictors available under L_1 , then the best achievable validation NLL under L_2 is no worse than under L_1 —an instance of the “more information cannot hurt” principle [31–33]. This motivates retaining at least one layer with an effectively unbounded horizon, so every token can attend to all preceding tokens and piece-level structure is preserved.

Second, deterministic deep processing cannot improve the Bayes-optimal log-loss. Let X denote the context, Y the prediction target, and $Z = g(X)$ a deterministic representation of X . Then $Y \rightarrow X \rightarrow Z$ forms a Markov chain, so by the data-processing inequality $H(Y | X) \leq H(Y | Z)$ [34]: the best achievable NLL using Z alone cannot beat that using the full context X . Any realized improvement from deeper representations must therefore come from inductive bias or optimization effects, not from surpassing the information limit [33, 34].

Consistent with this analysis, our experiments show that retaining long context at a shallower layer slightly outperforms retaining it at a deeper one. This helps explain why two-scale DSMR, which concentrates long horizons in lower layers, is the best-performing schedule in our setting.

6.2. State staleness and optimization stability

Because DSMR uses truncated backpropagation with a stop-gradient across segments (Eq. (4)), later segments condition on cached states produced under slightly older parameters. In our setting, each piece spans at most $T \leq \lceil 32768/s \rceil = 32$ recurrent steps (where $s=1024$ is the segment length), while training runs for roughly 3M optimizer steps; the step-to-step parameter mismatch over the cached history is therefore small. Empirically, extending the recurrence horizon beyond 30 segments—substantially longer than the effective history in the original Transformer-XL experiments [9]—does not degrade convergence.

This behavior is consistent with bounded staleness in pipelined and asynchronous optimization, where delayed parameter versions remain stable under controlled updates [18, 19, 35]. Under Adam-style optimization, the per-step parameter change is small, so the discrepancy between stale and freshly recomputed states behaves as a first-order perturbation rather than systematic bias. This stability provides a practical foundation for end-to-end full-piece training with long-horizon recurrence.

6.3. Practical implications for long-context music modeling

DSMR is designed around creator-centric, resource-limited workflows: depth-wise horizon budgeting keeps full-piece end-to-end training viable on consumer-grade hardware. This is relevant to music applications with tight hardware limits, such as interactive composition tools and rehearsal-time assistance. A representative scenario is real-time improvisational interaction, where the system uses a musician’s just-played phrase as a primer and generates a responsive continuation for turn-taking or call-and-response—a workflow common in jazz performance. Such settings often require models to run on portable devices, where the memory and throughput savings demonstrated by DSMR are directly beneficial. We note, however, that our evaluation uses offline teacher-forced perplexity; validating DSMR in real-time generation settings remains future work.

6.4. Limitations

Our findings are bounded by the regimes explored. (i) Validation PPL is teacher-forced and may not fully reflect long-range structural generation quality; no listening test or perceptual evaluation is conducted. (ii) Experiments use a single dataset (MAESTRO) and a single instrument (piano); conclusions about layer substitutability and depth placement may not generalize to other musical genres, ensemble textures, or non-music domains. (iii) We evaluate only one model scale ($L=18$, $d=1024$); the optimal horizon schedule may differ at larger or smaller capacities. (iv) No comparison is made against non-recurrent long-context methods (e.g., sparse attention trained on full pieces).

7. Conclusion

We presented **Depth-Structured Music Recurrence (DSMR)**, a training-time design that enables full-piece symbolic music modeling by streaming complete compositions left-to-right with stateful recurrent attention under a fixed layer-wise horizon budget. On MAESTRO, a **two-scale DSMR** schedule—long horizons in lower layers, a uniform short horizon elsewhere—matches the full-memory reference in perplexity (5.96 vs. 5.98) while using 59% less GPU memory and achieving 36% higher throughput. Variant analyses reveal strong layer substitutability under binary-horizon schedules and show that gate-derived layer rankings do not transfer reliably under structural intervention. Information-theoretically, these findings align with the principle that longer context cannot worsen optimal log-loss and that deterministic deep processing cannot surpass the Bayes limit, supporting the design choice of concentrating long-range access at shallow layers.

Future work includes evaluating DSMR under more extreme capacity bottlenecks and at larger model scales, assessing perceptual generation quality through listening tests, and testing DSMR on other modalities and long-context domains where stateful recurrent attention is relevant.

Appendix A. Stateful Recurrence and Long-Context Attention Approximations

This appendix formalizes Transformer-XL style stateful recurrence and clarifies how recurrent KV caching approximates segment-wise full attention in the forward pass. It further draws a connection to Perceiver AR as a stateless long-KV / short-Q analogue, highlighting a shared view of long-context handling via modifications at the attention interface.

Appendix A.1. Transformer-XL style stateful recurrence

We split a long sequence $x_{1:n}$ into segments of length s . The t -th segment is denoted by $x_t := (x_{(t-1)s+1}, \dots, x_{ts}) \in \mathcal{V}^s$. Let $H_t^{(0)} = \text{Embed}(x_t) \in \mathbb{R}^{s \times d}$ be token embeddings (including positional/relative positional encoding), and let $H_t^{(\ell)} \in \mathbb{R}^{s \times d}$ be the output of layer $\ell \in \{1, \dots, L\}$.

Transformer-XL maintains a per-layer KV memory from previous segments [9] (Fig. Appendix A.1). Let $M_{t-1}^{(\ell)} \in \mathbb{R}^{m \times d}$ be the memory used at layer ℓ for segment t (memory length m). When computing self-attention in layer ℓ , it concatenates historical memory and current hidden states:

$$\tilde{H}_t^{(\ell-1)} = [\text{SG}(M_{t-1}^{(\ell-1)}); H_t^{(\ell-1)}] \in \mathbb{R}^{(m+s) \times d}, \quad (\text{Appendix A.1})$$

where $\text{SG}(\cdot)$ denotes stop-gradient and $[\cdot; \cdot]$ is concatenation along the sequence dimension. Then layer ℓ applies a standard Transformer block:

$$H_t^{(\ell)} = \text{Block}^{(\ell)}(H_t^{(\ell-1)}, \tilde{H}_t^{(\ell-1)}), \quad (\text{Appendix A.2})$$

where keys/values come from $\tilde{H}_t^{(\ell-1)}$ and queries come from $H_t^{(\ell-1)}$ (Fig. Appendix A.1).

Memory is updated by keeping the most recent m token states (Eq. (1)).

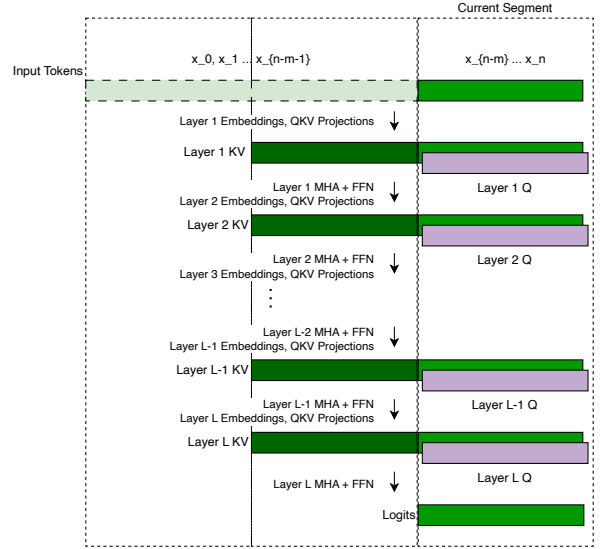


Figure Appendix A.1: Transformer-XL style stateful recurrence with stop-gradient KV memory. At each layer, keys/values (green) concatenate cached history with the current segment, while queries (purple) are computed for the current segment only.

Appendix A.2. How recurrence approximates segment-wise full attention

Consider full attention on the concatenation of all historical and current tokens. Focusing on queries from segment t , with historical keys/values ($K_{<t}, V_{<t}$) and current ones (K_t, V_t), full attention is

$$\text{Attr}(Q_t, [K_{<t}; K_t], [V_{<t}; V_t]). \quad (\text{Appendix A.3})$$

Stateful recurrence approximates Eq. (Appendix A.3) by caching historical activations so the model need not recompute the entire prefix at each step. With untruncated memory, $M_{t-1}^{(\ell-1)}$ supplies historical representations as keys/values together with the current segment (Eqs. (Appendix A.1)–(Appendix A.2)), yielding the same forward-pass form as Eq. (Appendix A.3). As illustrated in Fig. Appendix A.2, the concatenated KV source $[M_{t-1}^{(\ell-1)}; H_t^{(\ell-1)}]$ plays the same role as $[K_{<t}; K_t]$ (and likewise for values), matching Eq. (Appendix A.3) in the forward pass. Training, however, differs from true full attention due to stop-gradient through memory and statefulness: historical states consumed at step t are cached activations computed using parameters from earlier optimization steps and treated as constants, which shapes how long-range capability is learned under fixed budgets.

Appendix A.3. Perceiver AR as a stateless long-KV / short-Q analogue

Perceiver AR is not a stateful recurrent Transformer, but its first attention stage exhibits a similar long-KV / short-Q pattern to Transformer-XL-style recurrence [30]. Specifically, Perceiver AR uses a causally masked input cross-attention that maps a long input sequence into a much shorter latent array,

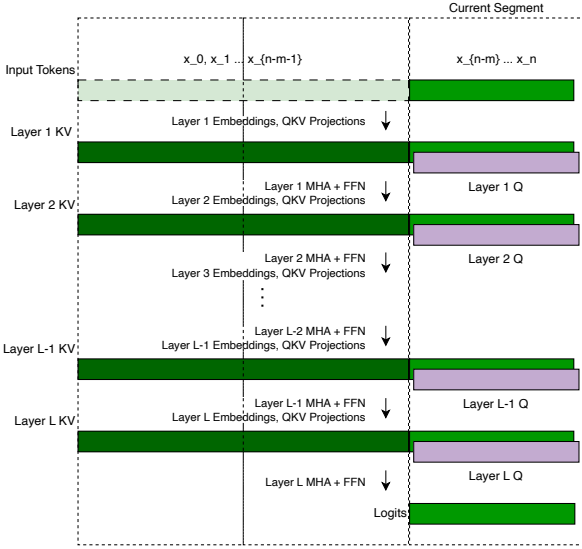


Figure Appendix A.2: **Segment-wise full attention view**. For queries from the current segment, full attention uses keys/values from both the historical prefix and the current segment (Eq. (Appendix A.3)). See Fig. Appendix A.1 for the stateful recurrence implementation that approximates this form in the forward pass when memory is untruncated.

typically aligning one latent with each of the final N input positions. Let $E_{1:T} \in \mathbb{R}^{T \times d}$ be input embeddings and $Z \in \mathbb{R}^{N \times d}$ be the latent queries. The cross-attention can be written abstractly as

$$\begin{aligned} \text{Attr}(Q_{\text{lat}}, K_{\text{in}}, V_{\text{in}}), \\ Q_{\text{lat}} = ZW_Q, \\ K_{\text{in}} = E_{1:T}W_K, \\ V_{\text{in}} = E_{1:T}W_V. \end{aligned} \quad (\text{Appendix A.4})$$

with a causal mask that prevents a latent aligned to position i from attending to inputs $> i$. This resembles recurrent attention in that queries are computed for a short set of positions (length N) while attending over a much longer KV context (length T), analogous to using long-range KV only at a shallow stage.

The key difference is statefulness. In Transformer-XL-style recurrence, the long-range KV comes from cached hidden states carried across segments (and detached via stop-gradient), whereas in Perceiver AR the long-range KV is formed by projecting the current input sequence embeddings at each forward pass (stateless), with causality enforced by masking. Figure Appendix A.3 illustrates the analogy.

Summary: near-vanilla architectures with attention-level context reduction

Despite differences in statefulness and implementation, Transformer-XL style recurrence and Perceiver AR both remain close to a vanilla Transformer in that the core Transformer blocks are preserved. Long-context handling is largely realized by changing how attention receives context: recurrence reuses cached hidden states as long-range KV (stateful, with stop-gradient), whereas Perceiver AR forms long-range KV from

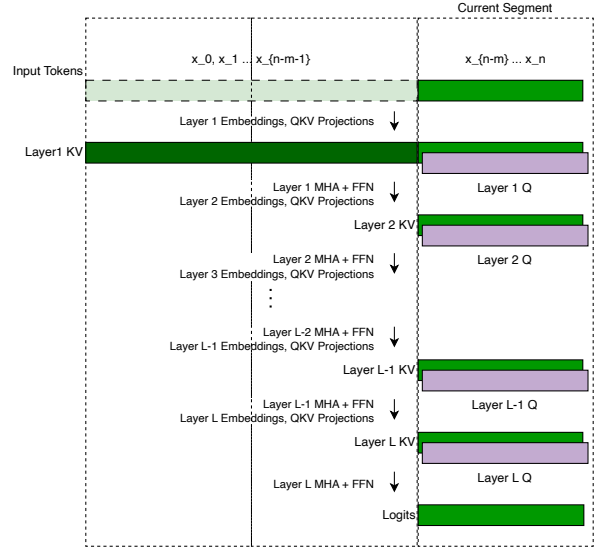


Figure Appendix A.3: **Perceiver AR as long-KV / short-Q cross-attention** [30]. A causally masked cross-attention maps a long input (projected embeddings as keys/values) to a short latent array (queries), after which a deep stack of self-attention operates only on the short latents. This is analogous to exposing long-range KV to an early stage, but differs from recurrent Transformers in that the KV is stateless (recomputed each pass) rather than cached recurrent state.

projected input embeddings and restricts computation through a short latent query set (stateless, with causal masking). In both cases, the effective context processed per step is reduced at the attention interface compared with full attention over the entire prefix, while maintaining the standard Transformer computation within each block.

Acknowledgements

AI-Assisted Language Editing. During the preparation of this work the authors used ChatGPT in order to improve English grammar and readability. After using this tool, the authors reviewed and edited the content as needed and take full responsibility for the content of the published article.

References

- [1] C.-Z. A. Huang, A. Vaswani, J. Uszkoreit, I. Simon, C. Hawthorne, N. Shazeer, A. M. Dai, M. D. Hoffman, M. Dinculescu, D. Eck, Music Transformer: generating music with long-term structure, in: International Conference on Learning Representations (ICLR), 2019, arXiv:1809.04281. doi:10.48550/arXiv.1809.04281.
- [2] B. Yu, P. Lu, R. Wang, W. Hu, X. Tan, W. Ye, S. Zhang, T. Qin, T.-Y. Liu, Museformer: Transformer with fine- and coarse-grained attention for music generation, in: Advances in Neural Information Processing Systems, Vol. 35, Curran Associates, Inc., 2022, pp. 1376–1388.
- [3] A. Vaswani, N. Shazeer, N. Parmar, J. Uszkoreit, L. Jones, A. N. Gomez, L. Kaiser, I. Polosukhin, Attention is all you need, in: Advances in Neural Information Processing Systems, Vol. 30, 2017, pp. 5998–6008, arXiv:1706.03762 [cs.CL]. doi:10.48550/arXiv.1706.03762.
- [4] R. Child, S. Gray, A. Radford, I. Sutskever, Generating long sequences with sparse transformers, arXiv:1904.10509 [cs.LG] (2019). doi:10.48550/arXiv.1904.10509.

- [5] I. Beltagy, M. E. Peters, A. Cohan, Longformer: the long-document transformer, arXivArXiv:2004.05150 [cs.CL] (2020). doi:10.48550/arXiv.2004.05150.
- [6] A. Katharopoulos, A. Vyas, N. Pappas, F. Fleuret, Transformers are RNNs: fast autoregressive transformers with linear attention, in: Proceedings of the 37th International Conference on Machine Learning (ICML), 2020, pp. 5156–5165, arXiv:2006.16236. doi:10.48550/arXiv.2006.16236.
- [7] A. Gu, T. Dao, Mamba: linear-time sequence modeling with selective state spaces, in: Proceedings of the First Conference on Language Modeling (COLM), 2024, arXiv:2312.00752. doi:10.48550/arXiv.2312.00752.
- [8] H. Ding, Z. Wang, G. Paolini, V. Kumar, A. Deoras, D. Roth, S. Soatto, Fewer truncations improve language modeling, in: Proceedings of the 41st International Conference on Machine Learning (ICML), 2024, pp. 11030–11048.
- [9] Z. Dai, Z. Yang, Y. Yang, J. G. Carbonell, Q. V. Le, R. Salakhutdinov, Transformer-XL: attentive language models beyond a fixed-length context, in: Proceedings of the 57th Annual Meeting of the Association for Computational Linguistics (ACL), 2019, pp. 2978–2988. doi:10.18653/v1/P19-1285.
- [10] C. Hawthorne, A. Stasyuk, A. Roberts, I. Simon, C.-Z. A. Huang, S. Dieleman, E. Elsen, J. H. Engel, D. Eck, Enabling factorized piano music modeling and generation with the MAESTRO dataset, in: International Conference on Learning Representations (ICLR), 2019, arXiv:1810.12247. doi:10.48550/arXiv.1810.12247.
- [11] M. Zaheer, G. Guruganesh, K. A. Dubey, J. Ainslie, C. Alberti, S. Ontañón, P. Pham, A. Ravula, Q. Wang, L. Yang, A. Ahmed, Big Bird: transformers for longer sequences, in: Advances in Neural Information Processing Systems, Vol. 33, 2020, arXiv:2007.14062. doi:10.48550/arXiv.2007.14062.
- [12] K. M. Choromanski, V. Likhoshesterov, D. Dohan, X. Song, A. Gane, T. Sarlós, P. Hawkins, J. Q. Davis, A. Mohiuddin, L. Kaiser, D. B. Belanger, L. J. Colwell, A. Weller, Rethinking attention with performers, in: International Conference on Learning Representations (ICLR), 2021, arXiv:2009.14794. doi:10.48550/arXiv.2009.14794.
- [13] A. Behrouz, P. Zhong, V. Mirrokni, Titans: learning to memorize at test time, in: Advances in Neural Information Processing Systems, 2025.
- [14] DeepSeek-AI, DeepSeek-V3.2: pushing the frontier of open large language models, arXivArXiv:2512.02556 [cs.CL] (2025). doi:10.48550/arXiv.2512.02556.
- [15] J. W. Rae, A. Potapenko, S. M. Jayakumar, C. Hillier, T. P. Lillcrap, Compressive transformers for long-range sequence modelling, in: International Conference on Learning Representations (ICLR), 2020, arXiv:1911.05507. doi:10.48550/arXiv.1911.05507.
- [16] A. Bulatov, Y. Kuratov, M. S. Burtsev, Recurrent memory transformer, in: Advances in Neural Information Processing Systems, 2022.
- [17] S. Ding, J. Shang, S. Wang, Y. Sun, H. Tian, H. Wu, H. Wang, ERNIE-Doc: a retrospective long-document modeling transformer, in: Proceedings of the 59th Annual Meeting of the Association for Computational Linguistics and the 11th International Joint Conference on Natural Language Processing (ACL/IJCNLP), 2021, pp. 2914–2927. doi:10.18653/v1/2021.ac1-long.227.
- [18] D. Narayanan, A. Harlap, A. Phanishayee, V. Seshadri, N. R. Devanur, G. R. Ganger, P. B. Gibbons, M. Zaharia, PipeDream: generalized pipeline parallelism for DNN training, in: Proceedings of the 27th ACM Symposium on Operating Systems Principles (SOSP), 2019, pp. 1–15. doi:10.1145/3341301.3359646.
- [19] W. Zhang, S. Gupta, X. Lian, J. Liu, Staleness-aware Async-SGD for distributed deep learning, in: Proceedings of the 25th International Joint Conference on Artificial Intelligence (IJCAI), 2016, pp. 2350–2356.
- [20] A. Liu, J. Liu, Z. Pan, Y. He, R. Haffari, B. Zhuang, MiniCache: KV cache compression in depth dimension for large language models, in: Advances in Neural Information Processing Systems, 2024.
- [21] Z. Wang, B. Cui, S. Gan, SqueezeAttention: 2D management of KV-cache in LLM inference via layer-wise optimal budget, in: International Conference on Learning Representations (ICLR), 2025.
- [22] Y. Shen, S. Yuan, Z. Zhang, X. Wang, D. Jiang, C.-T. Nguyen, LAVA: layer-wise KV cache eviction with dynamic budget allocation, in: Findings of the Association for Computational Linguistics: EMNLP 2025, 2025, pp. 13672–13692.
- [23] J. W. Rae, A. Razavi, Do transformers need deep long-range memory?, in: Proceedings of the 58th Annual Meeting of the Association for Computational Linguistics (ACL), 2020, pp. 7524–7529. doi:10.18653/v1/2020.ac1-main.672.
- [24] Z. Wang, L. Min, G. Xia, Whole-song hierarchical generation of symbolic music using cascaded diffusion models, in: International Conference on Learning Representations (ICLR), 2024.
- [25] X. Qu, Y. Bai, Y. Ma, Z. Zhou, K. M. Lo, J. Liu, R. Yuan, L. Min, X. Liu, T. Zhang, X. Du, S. Guo, Y. Liang, Y. Li, S. Wu, J. Zhou, T. Zheng, Z. Ma, F. Han, W. Xue, G. Xia, E. Benetos, X. Yue, C. Lin, X. Tan, W. Huang, J. Fu, G. Zhang, MuPT: a generative symbolic music pre-trained transformer, in: International Conference on Learning Representations (ICLR), 2025.
- [26] Y. Wang, S. Wu, J. Hu, X. Du, Y. Peng, Y. Huang, S. Fan, X. Li, F. Yu, M. Sun, NotaGen: advancing musicality in symbolic music generation with large language model training paradigms, in: Proceedings of the Thirty-Fourth International Joint Conference on Artificial Intelligence (IJCAI), 2025, pp. 10207–10215. doi:10.24963/ijcai.2025/1134.
- [27] Y. Zhao, Y. Qu, K. Staniszewski, S. Tworkowski, W. Liu, P. Miłoś, Y. Wu, P. Minervini, Analysing the impact of sequence composition on language model pre-training, in: Proceedings of the 62nd Annual Meeting of the Association for Computational Linguistics (ACL), 2024, pp. 7897–7912. doi:10.18653/v1/2024.ac1-long.427.
- [28] Y. Bengio, N. Léonard, A. C. Courville, Estimating or propagating gradients through stochastic neurons for conditional computation, arXivArXiv:1308.3432 [cs.LG] (2013). doi:10.48550/arXiv.1308.3432.
- [29] M. Courbariaux, Y. Bengio, J.-P. David, BinaryConnect: training deep neural networks with binary weights during propagations, in: Advances in Neural Information Processing Systems, Vol. 28, 2015, pp. 3123–3131.
- [30] C. Hawthorne, A. Jaegle, C. Cangea, S. Borgeaud, C. Nash, M. Malinowski, S. Dieleman, O. Vinyals, M. M. Botvinick, I. Simon, H. Sheahan, N. Zeghidour, J.-B. Alayrac, J. Carreira, J. H. Engel, General-purpose, long-context autoregressive modeling with Perceiver AR, in: Proceedings of the 39th International Conference on Machine Learning (ICML), Vol. 162 of Proceedings of Machine Learning Research, PMLR, 2022, pp. 8535–8558.
- [31] D. Blackwell, Equivalent comparisons of experiments, The Annals of Mathematical Statistics 24 (2) (1953) 265–272. doi:10.1214/aoms/1177729032.
- [32] A. P. Dawid, Statistical theory—the prequential approach (with discussion), Journal of the Royal Statistical Society: Series A (General) 147 (2) (1984) 278–292.
- [33] T. Gneiting, A. E. Raftery, Strictly proper scoring rules, prediction, and estimation, Journal of the American Statistical Association 102 (477) (2007) 359–378. doi:10.1198/016214506000001437.
- [34] T. M. Cover, J. A. Thomas, Elements of information theory, 2nd Edition, Wiley, Hoboken, NJ, 2006.
- [35] A. Kossou, V. Chiley, A. Venigalla, J. Hestness, U. Köster, Pipelined backpropagation at scale: training large models without batches, in: Proceedings of Machine Learning and Systems (MLSys), 2021.